

Influence of mass polydispersity on dynamics of simple liquids and colloids

N. Kiriushcheva^{1,*} and Peter H. Poole²

¹*Department of Physics and Astronomy, University of Western Ontario, London, Ontario N6A 3K7, Canada*

²*Department of Applied Mathematics, University of Western Ontario, London, Ontario N6A 5B7, Canada*

(Dated: November 5, 2018)

We conduct molecular dynamics computer simulations of a system of Lennard-Jones particles, polydisperse in both size and mass, at a fixed density and temperature. We test for and quantify systematic changes in dynamical properties that result from polydispersity, by measuring the pair distribution function, diffusion coefficient, velocity autocorrelation function, and non-Gaussian parameter, as a function of the degree of polydispersity. Our results elucidate the interpretation of experimental studies of collective particle motion in colloids, and we discuss the implications of polydispersity for observations of dynamical heterogeneity, in both simulations of simple liquids and colloid experiments.

PACS numbers: 05.20.Jj, 66.10.-x, 82.70.Dd

I. INTRODUCTION

The dynamical behavior of liquids is an area of intense current interest. Much of this interest has been motivated by the desire to understand the progressively slower and more complex dynamics of dense, supercooled liquids as they are cooled toward the glass transition [1]. In the last few decades, numerous direct insights on dynamical motion in liquids have been obtained using molecular dynamics (MD) computer simulations, in which the spatial coordinates of particles as a function of time are calculated [2]. More recently, experimental studies of colloids have used confocal microscopy to track individual particles [3, 4, 5, 6], thus generating the same type of data on microscopic particle motions as is obtained from simulations. For studying the glass transition, simulations and colloid experiments therefore serve as important model systems in which the implications of theory can be directly tested.

In both simulations and colloid experiments, fluids have been studied in which the particle size is polydisperse. In simulations, size polydispersity is often introduced to prevent crystallization of the deeply supercooled liquid (see e.g. [7]). In colloid experiments, some degree of polydispersity is always present, and depends on the process by which colloid particles are produced. To characterize the polydispersity of colloids, the distribution $\theta(\sigma)$ of particle diameters σ is commonly found (or assumed) to be Gaussian:

$$\theta_G(\sigma) = \frac{1}{\delta\sqrt{2\pi}} \exp\left[-\frac{1}{2}\left(\frac{\sigma - \sigma_0}{\delta}\right)^2\right], \quad (1)$$

where σ_0 is the average particle diameter, and δ characterizes the width of the distribution [8]. Polydispersity can then be quantified by the value of the dimensionless parameter $c = \delta/\sigma_0$.

In most experimental studies of colloids (see e.g. [8]) a system is regarded as effectively monodisperse if $c < 0.05$. For many properties, such as the average liquid structure, this is a good approximation. However, dynamical properties, especially at the microscopic level, may depend sensitively on the nature of microscopic structural fluctuations, and so may be affected by even small polydispersities. In addition, size polydispersity in real colloids leads inevitably to a polydispersity of mass. However, some models of polydisperse liquids and colloids consist of systems in which particle size varies, but not particle mass [7, 9].

In this paper we seek to isolate and quantify the role of size and mass polydispersity on the dynamics of a simple liquid system, in particular to assess the need to incorporate mass polydispersity when simulating the dynamics of realistic systems having size polydispersity. To do so, we conduct MD simulations of a system of particles interacting via the Lennard-Jones (LJ) potential, polydisperse with respect to both mass and size, as a function of c . Our results show that a range of dynamical properties (the diffusion coefficient, the velocity autocorrelation function, and the non-Gaussian parameter) of a polydisperse fluid are systematically shifted from the corresponding monodisperse case. We discuss the implications of these results for observations of “dynamical heterogeneity” in simulations [9, 10] and in colloid experiments [5, 6].

II. POLYDISPERSE LENNARD-JONES LIQUID

Since our aim is to study generic effects of polydispersity on liquid dynamics, we chose the well-studied LJ potential to model interparticle interactions. The LJ potential is popular for simulations of simple liquids, and there exist many studies to which to compare our results.

In simulations of colloids, the colloidal particles are often modeled as hard spheres, and for many cases this a good approximation. However, interactions among colloidal particles can take other forms, and can be explic-

*Electronic address: nkiriusc@uwo.ca

itly controlled, for example, by attaching soluble polymer chains by one end to the particle surface to generate repulsion, or by adding nonadsorbing soluble polymers to the suspension to produce attraction [11]. Though the present work is motivated by the recent experiments studying the dynamics of colloidal particles, we do not address the question of how the behavior of a colloidal system depends on the shape of the interparticle interaction potential. We also do not take into account the influence of a solvent.

We perform equilibrium molecular dynamics simulations in three dimensions of a system of $N = 4000$ particles interacting via the shifted-force LJ potential, a modification of the standard LJ potential,

$$V_{ij}(r) = 4\varepsilon \left[\left(\frac{\sigma_{ij}}{r} \right)^{12} - \left(\frac{\sigma_{ij}}{r} \right)^6 \right]. \quad (2)$$

Here, V_{ij} is the potential of interaction of two particles i and j , separated by a distance r . ε characterizes the strength of the pair interaction and is constant for all particle pairs. In the shifted-force LJ interaction, the LJ potential and force are modified so as to go to zero continuously at $r = 2.5\sigma_0$, and interactions beyond $2.5\sigma_0$ are ignored [2].

Polydispersity is introduced through the particle size: $\sigma_{ij} = (\sigma_i + \sigma_j)/2$ where σ_i (σ_j) characterizes the diameter of a particle i (j). Particles are assigned σ values by random sampling from the Gaussian distribution in Eq. 1. We also impose a mass polydispersity appropriate for the given size polydispersity. The mass of a particle i is $m_i = m_0(\sigma_i/\sigma_0)^3$, where m_0 is the mass of a particle of size σ_0 . Particle trajectories are evaluated using the leap-frog Verlet algorithm [2], using the appropriate value of m_i in the equation of motion of each particle.

Throughout this work we use reduced units. Energy is expressed in units of ε , length in units of σ_0 , the number density of particles ρ in units of σ_0^{-3} , and temperature T in units of ε/k , where k is Boltzmann's constant. Time t is expressed in units of $\sqrt{m_0\sigma_0^2/\varepsilon}$. In these units the time step used for integrating the particle equations of motion is 0.01.

After equilibration, all quantities are evaluated in the microcanonical ensemble. We present data for $\rho = 0.75$ and $T = 0.66$, a state not far from the triple point of the monodisperse LJ fluid ($\rho = 0.85$, $T = 0.76$) [12, 13]. We chose this state point so as to avoid the dense, deeply supercooled liquid region of the phase diagram of the monodisperse LJ system, where spontaneous crystallization could interfere with the evaluation of equilibrium properties. We conduct separate simulations for $c = 0$, 0.05 and 0.1.

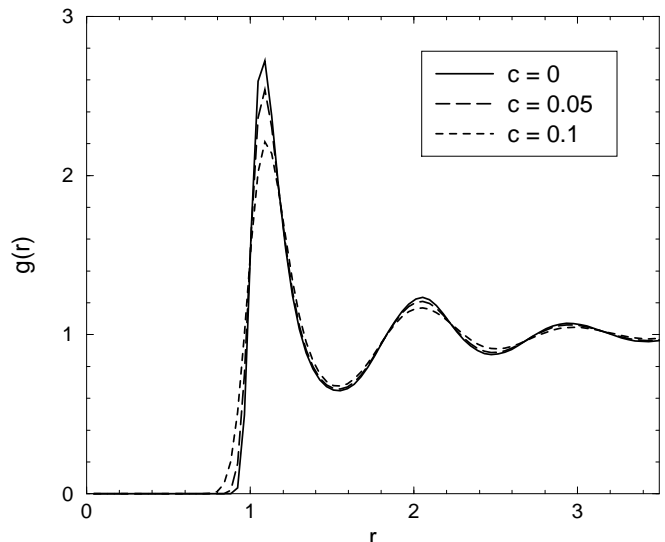


FIG. 1: Effect of polydispersity c on the average liquid structure as measured by $g(r)$.

III. PAIR DISTRIBUTION FUNCTION, DIFFUSION COEFFICIENT, AND VELOCITY AUTOCORRELATION FUNCTION

The pair distribution function $g(r)$ that characterizes the average liquid structure [14] is shown in Fig. 1 for each c studied. The effect of increasing polydispersity is to reduce the height of, and broaden the peaks associated with the successive neighbor shells around each particle. However the mean position of each neighbor shell does not change noticeably.

We test for a dependence on c of the bulk transport properties by evaluating the diffusion coefficient D . We obtain D from $\langle r^2(t) \rangle$ using the Einstein relation,

$$D = \lim_{t \rightarrow \infty} \frac{\langle r^2(t) \rangle}{6t}. \quad (3)$$

Fig. 2 shows the dependence of D on c . We find that at fixed ρ and T , D decreases systematically by about 10% as c increases from zero to 0.1.

Fig. 3 shows the dependence on c of the velocity autocorrelation function $\psi(t)$ [13]:

$$\psi(t) = \frac{\langle \mathbf{v}(0) \cdot \mathbf{v}(t) \rangle}{\langle |\mathbf{v}|^2 \rangle}, \quad (4)$$

where $\mathbf{v}(t)$ is the velocity of a particle at time t . D is related to the integral of $\psi(t)$, and consistent with the decrease of D , the negative part of $\psi(t)$ becomes larger in magnitude with increasing c . This trend reflects an increase with c of the strength with which single particle dynamical properties of the system are retained on a time scale comparable to the collision time.

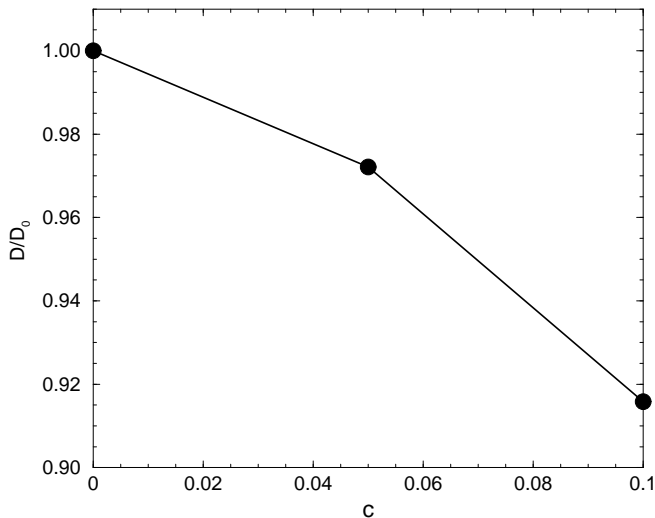


FIG. 2: Fractional deviation with c of D relative to D_0 , its value for a perfectly monodisperse system.

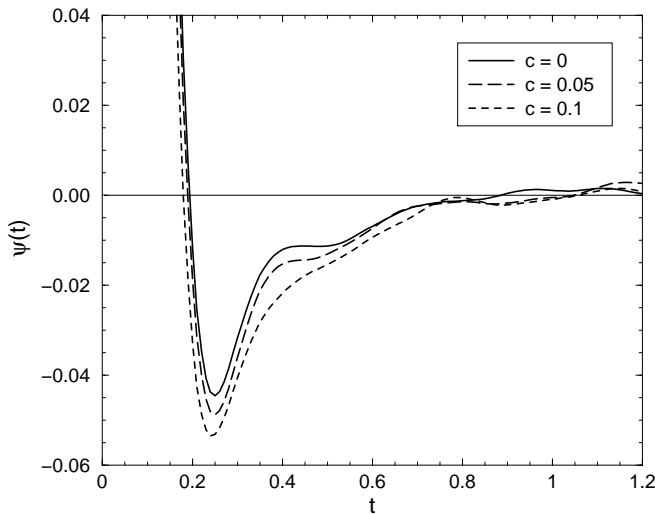


FIG. 3: Effect of polydispersity c on the velocity autocorrelation function, $\psi(t)$.

IV. NON-GAUSSIAN PARAMETER

The general non-Gaussian parameter $\alpha_n(t)$ is defined for integers $n \geq 1$ as [13],

$$\alpha_n(t) = \frac{\langle r^{2n}(t) \rangle}{c_n \langle r^2(t) \rangle^n} - 1, \quad (5)$$

where $c_n = [1 \cdot 3 \cdot 5 \cdots (2n+1)]/3^n$. $\langle r^{2n}(t) \rangle$ is the ensemble average of the $2n^{\text{th}}$ power of the particle displacements after a time t [15]:

$$\langle r^{2n}(t) \rangle = \left\langle \frac{1}{N} \sum_{i=1}^N |\mathbf{r}_i(t) - \mathbf{r}_i(0)|^{2n} \right\rangle. \quad (6)$$

Here, $\mathbf{r}_i(t)$ denotes the position of particle i after a time t following a reference time $t = 0$ in equilibrium. N is the total number of particles in the system.

The functions $\langle r^{2n}(t) \rangle$ also represent the even moments of $G_s(\mathbf{r}, t)$, the self-part of the van Hove correlation function [14]. For an isotropic fluid made up of particles with spherically symmetric interactions, we can restrict our attention to $G_s(r, t)$, the probability density that a particle located at the origin at time $t = 0$ will be found within dr of a distance r at time t [16]:

$$G_s(r, t) = \left\langle \frac{1}{N} \sum_{i=1}^N \delta(r - |\mathbf{r}_i(t) - \mathbf{r}_i(0)|) \right\rangle. \quad (7)$$

In terms of $G_s(r, t)$, $\langle r^{2n}(t) \rangle$ can be written,

$$\langle r^{2n}(t) \rangle = 4\pi \int_0^\infty r^{2n} G_s(r, t) r^2 dr. \quad (8)$$

In the case of an ideal gas of non-interacting particles having a Maxwell-Boltzmann velocity distribution [14], $G_s(r, t)$ is a Gaussian function of r :

$$G_s(r, t) = \left(\frac{\beta m}{2\pi t^2} \right)^{3/2} \exp\left(-\frac{\beta m r^2}{2t^2}\right), \quad (9)$$

where $\beta = 1/kT$. In this case, it is readily shown that $\langle r^{2n}(t) \rangle = c_n \langle r^2(t) \rangle^n$ and so $\alpha_n(t) = 0$. For systems in which correlations of particle motions are prominent, $G_s(r, t)$ is not Gaussian, and the deviation of $\alpha_n(t)$ from zero serves to quantify the deviation of $G_s(r, t)$ from the Gaussian form.

In the present work we present results for $\alpha_2(t)$, the most commonly calculated non-Gaussian parameter:

$$\alpha_2(t) = \frac{3\langle r^4(t) \rangle}{5\langle r^2(t) \rangle^2} - 1. \quad (10)$$

In Fig. 4 we plot $\alpha_2(t)$ for three different values of polydispersity $c = 0, 0.05$ and 0.1 . Qualitatively, there are two effects induced by increasing polydispersity: (i) the characteristic, intermediate-time peak of α_2 , at approximately $t = 1$, increases in magnitude as c increases; and, (ii) the value of $\alpha_2(t)$ does not start from zero in the limit $t \rightarrow 0$ when $c \neq 0$. We clarify each of these effects in turn below.

To distinguish the influence of mass and size polydispersity separately, we conduct two new simulations, one (“size-only”) for a system in which the size polydispersity is $c = 0.1$, but in which all the particle masses are set equal to m_0 ; and another (“mass-only”) for which the mass polydispersity is taken from our previous “mass-and-size” $c = 0.1$ case, but with all the particle sizes then set equal to σ_0 . We compare in Fig. 5 the resulting behavior of α_2 as a function of t with the behavior found for the monodisperse $c = 0$ case; and with the case where both size and mass are polydisperse with $c = 0.1$.

First we focus on the behavior observed near the maximum of $\alpha_2(t)$ at approximately $t = 1$. Although the

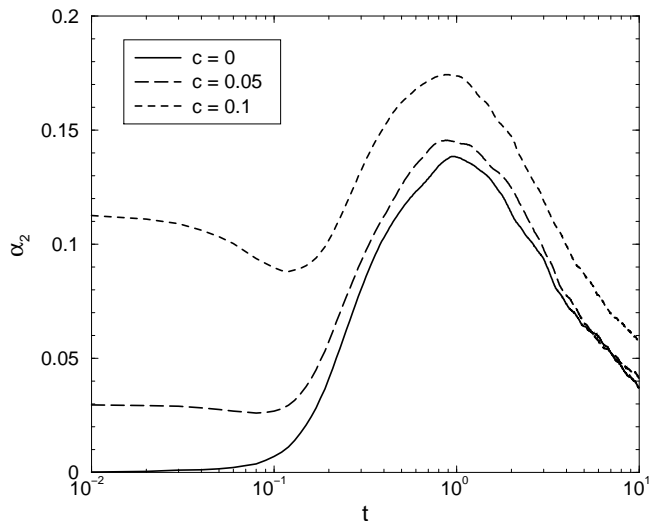


FIG. 4: Variation of $\alpha_2(t)$ with c .

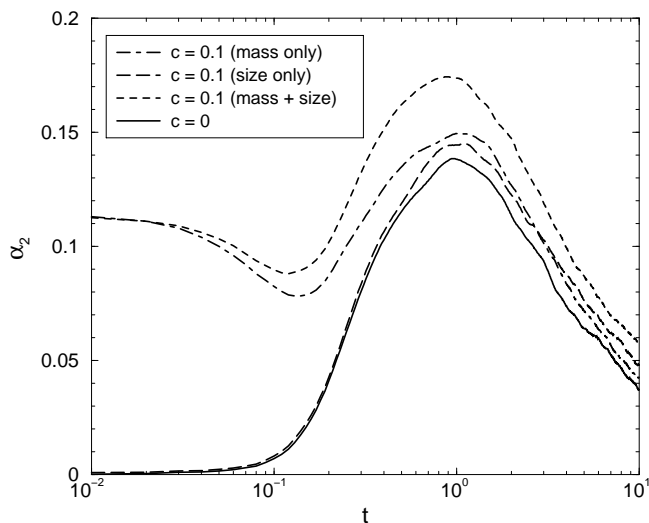


FIG. 5: $\alpha_2(t)$ for several types of polydispersity, demonstrating that polydispersity of both particle size and mass has a greater impact, compared to the monodisperse case, than either size-only or mass-only polydispersity.

mass-only curve in Fig. 5 lies above that of the monodisperse system, it still lies well below that corresponding to polydispersity of both mass and size. Hence, mass polydispersity is not solely responsible for the increase of the maximum of α_2 with c . Interestingly, the size-only curve is also well below that corresponding to polydispersity of both mass and size. Even the sum of the deviations from the monodisperse case of the mass-only and size-only curves, is insufficient to account for the height of the curve for the system with polydispersity of both mass and size. That is, polydispersity of both mass and size together has a greater impact on dynamical properties at intermediate times than can be obtained from

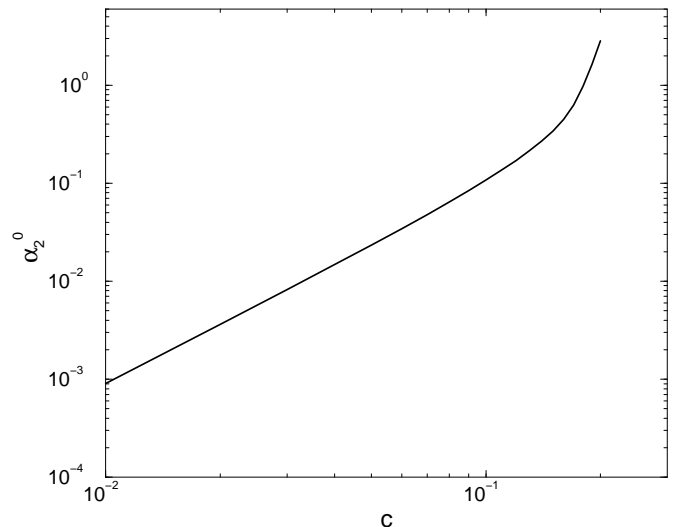


FIG. 6: Log-log plot of α_2^0 as a function of c for a Gaussian distribution of particle diameters.

polydispersity of mass or size alone.

Next we turn our attention to the behavior of α_2 as $t \rightarrow 0$. (For the remainder of this work we will denote the limit as $t \rightarrow 0$ of α_2 as α_2^0 .) In MD simulations of a one-component LJ system [15, 17] and of a binary LJ mixture [7, 10], $\alpha_2^0 = 0$. However, in the binary LJ mixture studied, the two species differ in size only and have the same mass, in contrast to our system in which the masses of particles differ in accordance with the polydispersity of their sizes. Two of the curves in Fig. 5 ($c = 0$ and “size-only”) correspond to systems with no mass polydispersity, and in both cases $\alpha_2^0 = 0$. For the other two curves ($c = 0.1$ and “mass-only”), α_2^0 adopts the same nonzero value. It is clear that the mass polydispersity is solely responsible for the behavior of α_2^0 .

As $t \rightarrow 0$, the atomic motions in the fluid correspond to those of free particles, and the distribution of velocities is the Gaussian function given in Eq. 9. For a monodisperse system, this means that $\alpha_2^0 = 0$. For a system with polydisperse masses, each particle of a given mass also samples the Gaussian velocity distribution given in Eq. 9. However, the Gaussian distributions sampled will have different widths for particles of different m . Consequently, the form of the total $G_s(r, t)$ function is not in general Gaussian because it is a superposition of individual Gaussians of different width. The result is a non-zero value of α_2^0 , as found in our simulations.

Since the limit $t \rightarrow 0$ corresponds to the free-particle limit for atomic motion, we can calculate the non-Gaussian parameter for a polydisperse system as $t \rightarrow 0$ exactly. Consider a system of N particles in which there are M species (labeled by index j) each having N_j particles of mass m_j . The moments $\langle r^{2n}(t) \rangle$ can be found using a modified form of Eq. 6 appropriate for an M -

component system:

$$\langle r^{2n}(t) \rangle = \left\langle \frac{1}{N} \sum_{j=1}^M \sum_{i=1}^{N_j} |\mathbf{r}_i(t) - \mathbf{r}_i(0)|^{2n} \right\rangle. \quad (11)$$

Eq. 11 can be rewritten as,

$$\langle r^{2n}(t) \rangle = \sum_{j=1}^M f_j \langle r^{2n}(t) \rangle_j, \quad (12)$$

where $f_j = N_j/N$ is the fraction of particles of species j and

$$\langle r^{2n}(t) \rangle_j = \left\langle \frac{1}{N_j} \sum_{i=1}^{N_j} |\mathbf{r}_i(t) - \mathbf{r}_i(0)|^{2n} \right\rangle, \quad (13)$$

where the sum is over particles only of species j . For each species, the atomic motion as $t \rightarrow 0$ is also described by Eq. 9 with the appropriate value of $m = m_j$, and hence, the moments $\langle r^2(t) \rangle_j$ and $\langle r^4(t) \rangle_j$ can be found in the limit $t \rightarrow 0$ by substituting Eq. 9 into Eq. 8 for each j . The result is,

$$\langle r^2(t) \rangle_j = \frac{3t^2}{\beta m_j}, \quad (14)$$

and,

$$\langle r^4(t) \rangle_j = \frac{15t^4}{\beta^2 m_j^2}. \quad (15)$$

The value of α_2° for the multicomponent system can then be found by using Eqs. 12, 14 and 15 in Eq. 10:

$$\alpha_2^\circ = \frac{\sum_{j=1}^M m_j^{-2} f_j}{\left(\sum_{j=1}^M m_j^{-1} f_j \right)^2} - 1 \quad (16)$$

This expression highlights that α_2° may not equal zero for a system with polydisperse masses.

If the polydispersity is expressed as a continuous distribution of masses $\phi(m)$, Eq. 16 generalizes to,

$$\alpha_2^\circ = \frac{\int_0^\infty m^{-2} \phi(m) dm}{\left(\int_0^\infty m^{-1} \phi(m) dm \right)^2} - 1. \quad (17)$$

Experimental studies of colloids typically characterize polydispersity not in terms of the masses, but in terms of the particle diameters, described by $\theta(\sigma)$. Assuming that the particle mass m is proportional to σ^3 , and that $\phi(m) dm = \theta(\sigma) d\sigma$, Eq. 17 becomes,

$$\alpha_2^\circ = \frac{\int_0^\infty \sigma^{-6} \theta(\sigma) d\sigma}{\left(\int_0^\infty \sigma^{-3} \theta(\sigma) d\sigma \right)^2} - 1. \quad (18)$$

Note that the value of α_2° therefore depends only on the shape of the mass distribution function, and is otherwise

constant for all choices of ρ , T and interparticle interaction.

We apply the above result to the case of the Gaussian distribution of particle diameters given in Eq. 1. We substitute $\theta = \theta_G$ with $\sigma_0 = 1$ in Eq. 18 and calculate α_2° as a function of c (Fig. 6). We evaluate the integrals in Eq. 18 numerically, replacing the limits of integration $(0, \infty)$ with $[0.01\sigma_0, 2\sigma_0]$. This avoids the divergence of the integrands at $\sigma = 0$, and in any case is more physical, since a real distribution of particle sizes would have a non-zero lower bound, and a finite upper bound. As seen in Fig. 6, $\alpha_2^\circ \propto c^2$ for small c , but increases more rapidly than this for $c > 0.1$. The predictions of Eq. 6 are in agreement with our simulation results. For $c = 0.05$ Eq. 18 gives $\alpha_2^\circ = 0.02344$, while our simulation gives $\alpha_2^\circ = 0.027$; for $c = 0.1$ we obtain $\alpha_2^\circ = 0.10781$ and 0.113 , respectively.

We can also use Eq. 18 to calculate α_2° for a system in which the distribution of sizes is not Gaussian. For example, Sear [18] simulated a system of hard spheres, polydisperse in both size and mass, using a ‘‘hat’’ function of width w : $\theta(\sigma) = (w\sigma_0)^{-1}$ for $\sigma_0(1 - w/2) \leq \sigma \leq \sigma_0(1 + w/2)$, and $\theta(\sigma) = 0$ otherwise, and $m \sim \sigma^3$. For this case, we are able to solve Eq. 18 exactly, giving,

$$\alpha_2^\circ = \frac{(1 + \omega/2)^5 - (1 - \omega/2)^5}{5\omega(1 - \omega^2/4)} - 1. \quad (19)$$

For $\omega = 0.3$, Eq. 19 gives $\alpha_2 = 0.06916$, while for $\omega = 0.7$, $\alpha_2 = 0.4222$, in agreement with the simulation results in Fig. 6 of Ref. [18].

V. DISCUSSION

When α_2 has been extracted via confocal microscopy in colloid experiments, values as high as $\alpha_2^\circ \approx 1.5$ have been observed [3, 4, 5]. In these studies the polydispersity ranged from $c = 0.01$ to 0.1 . Kasper, et al. [3] observed that α_2° is not zero for all values of the volume fraction occupied by the colloidal particles. Marcus, et al. [4] found that α_2° is nonzero and increases with increasing volume fraction. Weeks, et al. [5] found that α_2° is approximately constant for small volume fractions but grows for higher volume fractions. In general, α_2° was found to increase with the volume fraction occupied by the colloid particles, in contrast to the absence of any density dependence in Eq. 18. In the case of real colloids, the behavior of α_2 as $t \rightarrow 0$ is complicated by the fact that solvent-induced hydrodynamic forces among particles potentially introduce strong, short-time-scale correlations of particle velocities, invalidating the free-particle assumption that is the basis of Eq. 9. The large difference between the behavior of α_2° found for these systems, and that predicted by Eq. 18 demonstrates that polydispersity alone cannot account for the observed values of α_2° , and that hydrodynamic effects indeed dominate the short-time dynamical behavior of real colloids.

At intermediate times, we find that the peak value of α_2 increases with c . The maximum value of α_2 has been shown [10] to correlate to the degree of dynamical heterogeneity present in the system: that is, transient, spatially correlated groups of particles whose characteristic structural relaxation time differs from the mean. Our results therefore suggest that dynamical heterogeneity, prominently observed at lower T and higher ρ than studied here, may be enhanced as polydispersity increases. One source of this enhancement may be the influence of mass polydispersity on spontaneously occurring density fluctuations, that in turn control the development of dynamical heterogeneities. In general, the occurrence and quantification of dynamical heterogeneity in a polydisperse system is likely to be more complicated than in a monodisperse (or even bi-disperse) system. At the same time, since we observe a slowing of the dynamics with increasing polydispersity, the dynamical heterogeneity may be more prominent and longer-lived in a polydisperse system, and so may facilitate the study of these complex structures.

In summary, we have illustrated that a system of particles with polydispersity of both mass and size is a more realistic model (compared to models without mass polydispersity) for studying the dynamics of colloids in MD simulations. Our results show that typical polydisper-

sities found in real systems can induce an influence of the order of 10% on dynamical properties. This is a small effect for studies, such as those near a glass transition, where relaxation times may vary by several orders of magnitude. At the same time, knowledge of the amount and direction of the impact of polydispersity on dynamics is required because polydispersity is so commonly found in systems studied both in simulations and experiments. This knowledge is also crucial for precise tests of theories, particularly those formulated for perfectly monodisperse systems. We also note that our results can be tested experimentally in colloids by deliberately varying the polydispersity of the studied colloidal system. Indeed, by varying c alone it might be possible to study an “isothermal-isochoric glass transition” (i.e. a glass transition at both fixed T and ρ) by setting up an appropriate series of colloidal systems where the polydispersity is progressively increased.

VI. ACKNOWLEDGMENTS

NK thanks Sergiy Kuzmin for valuable discussions. NK and PHP acknowledge financial support from NSERC (Canada).

-
- [1] M.D. Ediger, C.A. Angell and S.R. Nagel, *J. Phys. Chem.* **100**, 13200 (1996).
 - [2] M.P. Allen and D.J. Tildesley, *Computer Simulation of Liquids* (Clarendon, Oxford, 1987).
 - [3] A. Kasper, E. Bartsch and H. Sillescu, *Langmuir* **14**, 5004 (1998).
 - [4] A.H. Marcus, J. Schofield and S.A. Rice, *Phys. Rev. E* **60**, 5725 (1999).
 - [5] E.R. Weeks, J.C. Crocker, A.C. Levitt, A. Schofield and D.A. Weitz, *Science* **287**, 627 (2000).
 - [6] W.K. Kegel and A. van Blaaderen, *Science* **287**, 290 (2000).
 - [7] W. Kob and H.C. Andersen, *Phys. Rev. E* **51**, 4626 (1995).
 - [8] R.J. Hunter, *Foundations of Colloid Science* (Clarendon Press, Oxford, 1987), vol. 1.
 - [9] B. Doliwa and A. Heuer, *Phys. Rev. E* **61**, 6898 (2000).
 - [10] W. Kob, C. Donati, S.J. Plimpton, P.H. Poole and S.C. Glotzer, *Phys. Rev. Lett.* **79**, 2827 (1997).
 - [11] A.P. Gast and W.B. Russel, *Physics Today* **51**, 24 (1998).
 - [12] J.J. Nicolas, et al., *Mol. Phys.* **37** 1429 (1979).
 - [13] J.P. Boon and S. Yip, *Molecular Hydrodynamics* (Dover, New York, 1980).
 - [14] J.P. Hansen and I.R. McDonald, *Theory of Simple Liquids* (Academic, London, 1986).
 - [15] A. Rahman, *Phys. Rev.* **136**, 405 (1964).
 - [16] L. van Hove, *Phys. Rev.* **95**, 249 (1954).
 - [17] R.C. Desai, *J. Chem. Phys.* **44**, 77 (1966).
 - [18] R.P. Sear, *J. Chem. Phys.* **113**, 4732 (2000).